Symkom 2014 **Open Access**

Grzegorz Liśkiewicz* and Longin Horodko

Time-frequency analysis of the Surge Onset in the Centrifugal Blower

DOI 10.1515/eng-2015-0040

Received January 23, 2015; accepted June 16, 2015

Abstract: Time frequency analysis of the surge onset was performed in the centrifugal blower. A pressure signal was registered at the blower inlet, outlet and three locations at the impeller shroud. The time-frequency scalograms were obtained by means of the Continuous Wavelet Transform (CWT). The blower was found to successively operate in four different conditions: stable working condition, inlet recirculation, transient phase and deep surge. Scalograms revealed different spectral structures of aforementioned phases and suggest possible ways of detecting the surge predecessors.

Keywords: compressor; blower; surge; unstable flow; time-frequency; continuous wavelet transform; CWT

1 Introduction

1.1 Unstable flow structures in centrifugal compressing units

Whenever a compressing machine operates at a given rotational speed and the flow rate is continuously reduced, there is a moment after which the system will no longer operate in a stable manner. It is very important to accurately predict the point at which instabilities are likely to occur. However, there are many mechanisms and regions of appearance of unstable flow structures and it is very difficult to predict the conditions of their occurrence. Non-stable phenomena in centrifugal units were first identified and thoroughly analysed by Emmons *et al.* [1]. In 1976 Greitzer developed a mathematical model of instabilities [2] and confirmed it by experiment [3]. Apart from the fact that the Greitzer model was originally created for axial compressors, it was also successfully applied to describe the operation of centrifugal units [4]. Afterwards these findings were developed to describe the shape of fully-formed unstable flow phenomena [5, 6].

1.2 Classification of unstable flow structures

Each unstable flow structure is associated with oscillations of flow parameters which propagates in a certain direction. Direction of disturbance propagation can be treated as a good distinguishing mark for each class of unstable flow structures. Instability can be global and occupy the whole machine together with the inlet and the outlet piping or can appear locally. In the case of local instabilities the place of appearance is also important for classification. Each part of the compressing machine is characterized by different flow structures and consequently different unstable phenomena can be triggered therein [7]. Based on these criteria, the most common unstable flow structures can be distinguished, namely:

- Surge - global flow fluctuations in the axial direction [2, 3].
- Rotating Stall (RS) - local circumferential flow fluctuations. Depending on the place of occurrence it can be classified as:
  - Progressive Impeller Rotating Stall (PIRS) - appearing in the inducer zone. This structure is usually connected with gradual drop of the machine pressure ratio, hence the name "progressive" [8, 9].
  - Abrupt Impeller Rotating Stall (AIRS) - appearing close to the impeller outlet. This structure is usually connected with sudden drop of the machine pressure ratio, hence the name "abrupt" [10].
  - Vaneless Diffuser Rotating Stall (VDRS) - appearing in the diffuser [11, 12].
- Inlet Recirculation (IR, also known as the inducer recirculation or inducer backflow) - local flow structure upstream of the impeller. This phenomenon has a form of toroidal flow structure that can be present around the whole circumference [13, 14].

***Corresponding Author: Grzegorz Liśkiewicz:** Łódź University of Technology, Institute of Turbomachinery 90 - 924 Łódź, ul. Wólczańska 219/223, E-mail: grzegorz.liskiewicz@p.lodz.pl

Longin Horodko: Łódź University of Technology, Institute of Turbomachinery 90 - 924 Łódź, ul. Wólczańska 219/223

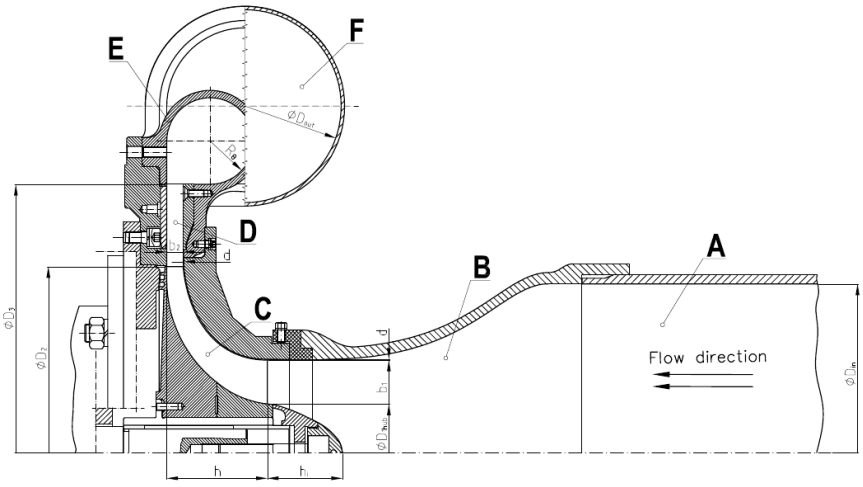

Figure 1: Cross-section of the DP1.12 blower used in this study with the most important dimensions.

1.3 Experimental analysis of the onset of the unstable phenomena

Dynamic tests are a very popular way of examining the surge onset in compressing machines. Such a method was applied in many papers including [15–18]. In this method, the mass flow rate was gradually decreased during signal collection. This is usually obtained by an increase of throttling which is normally done by gradual closure of the throttling valve. Dynamic signals were often subject to post-processing. Bulot *et al.* applied low-pass filter [18], while Lawless and Fleeter [16] used band-pass filter.

Another method includes examination of pressure signals registered for fixed throttling valve position in the frequency domain. It introduced new insight into the description of rotating stall and surge. As expected, comparison of frequency spectra at the design point to those attained at surge revealed the presence of new frequency components [19]. The number of local maxima in the spectra reflected the complexity of the non-stable flow structures. It is also possible to observe how the structures propagate throughout the unit by analysing frequency spectra at different working conditions in different locations. In this way Tamaki concluded that the stall inception takes place in the vicinity of rotor leading edge [20].

Time-frequency analysis combined advantages of the dynamic test and presentation of signals in the frequency domain. Horodko in his work used the continuous wavelet transform (CWT) to obtain time-dependent frequency spectra at the surge onset [17, 21, 22]. The study confirmed that the rotating stall initiates in the vicinity of the impeller leading edge. Similar phenomena were observed in other experiments conducted on different compressing units [15, 23, 24].

1.4 Scope of the study

Present study concerns the CWT analysis providing time-frequency signal characteristics during the surge and surge onset in the centrifugal blower. The analysed blower was designed to differ significantly from the ones which are present in literature. The examined machine is characterized by low specific speed, axial guideless inlet with Witoszynski nozzle [25] and vaneless diffuser.

2 Experimental procedure

2.1 Test stand description

A single stage centrifugal blower DP1.12 was the object of investigation. Figure 1 presents the cross-section of the blower and its main dimensions. The flow entered the rig through the inlet pipe (A) of diameter $D_{in} = 300.0$ mm. Then, it was accelerated in the Witoszynski nozzle [25] (B) and directed towards the impeller (C). The rotor inlet diameter at the hub equalled $D_{1hub} = 83.6$ mm and the inlet span $b_1 = 38.9$ mm. At the outlet, the diameter and the span equalled $D_2 = 330.0$ mm and $b_2 = 14.5$ mm respectively. The gap between the blade tip and the shroud maintained constant value $\delta = 0.8$ mm along the whole blade. Downstream of the rotor, air entered the vaneless diffuser (D). The diffuser outlet diameter was equal to $D_3 = 476.0$ mm. Afterwards, flow entered the circular volute (E). The radius was gradually increasing streamwise from the volute tongue gap of 5.0 mm towards the outlet pipe of diameter $D_{out} = 150.0$ mm. A throttling valve was mounted at the end of the outlet pipe of length $l = 5.5$ m. The volume of the outlet pipe was equal to

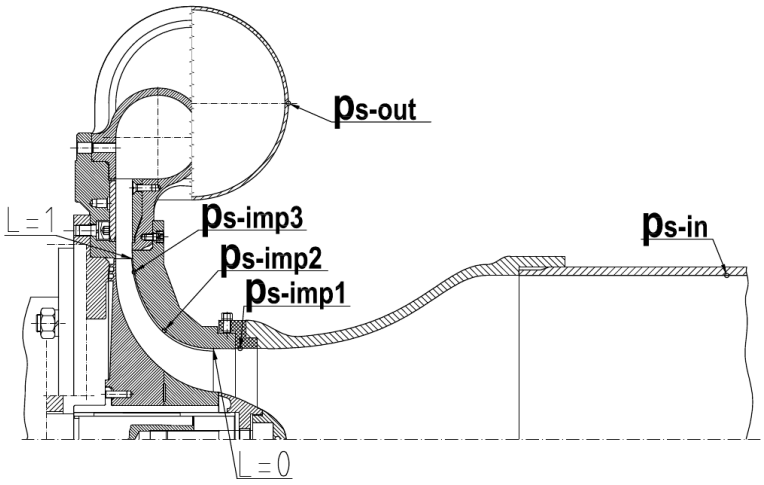

Figure 2: Cross-section of the DP1.12 blower used in this study with positions of the pressure gauges.

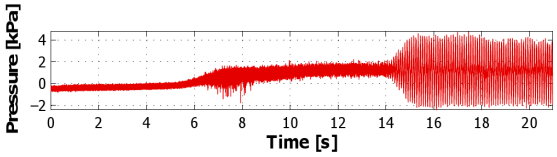

Figure 3: Pressure registered at gauge p_{s-imp1} during one of dynamic tests.

V_{out} = 0.0968 m^3 which corresponds to Helmholtz frequency of f_H = 11 Hz [26]. The rotor was driven by an asynchronous AC motor (400 V/15 kVA). The blower was designed to operate at ambient inlet conditions. The unit was run with rotational speed of f_{rot} = 100 Hz with nominal flow rate of $\acute{m}_n$ = 0.75 kg/s and pressure ratio PR = 1.08. Rotational speed yielded the impeller tip speed equal to u_{tip} = 103 m/s. The impeller had z = 23 blades, hence the blade passing frequency was equal to f_{BP} = 2.3 kHz.

The test stand was equipped with 5 dynamic Kulite transducers connected to an Iotech Wavebook 516/E data acquisition system. All transducers were mounted flush to the shroud walls to measure the static pressure. Gauge positions are presented in Figure 2. The list below contains the notation and position of each gauge:

- p_{s-in} - static pressure at the inlet pipe upstream of the Witoszynski nozzle;
- p_{s-out} - outlet static pressure at the volute outlet;
- p_{s-imp1} - static pressures at the impeller shroud, in the inlet zone (L = 0.2);
- p_{s-imp2} - static pressures at the impeller shroud, at the mid-chord (L = 0.4);
- p_{s-imp3} - static pressures at the impeller shroud, near the trailing edge (L = 0.9).

Longitudinal position of the static tappings at the impeller shroud was described with the L dimensionless parameter. It was set to be equal to L = 0 at the rotor leading edge and L = 1 at the rotor trailing edge.

2.2 Signal collection and analysis

Each signal measurement was conducted during the gradual closure of the throttling valve. The data series contained 2^{21} = 2097152 samples gathered with a frequency of 100 kHz . The signal was recorded continuously over 20.97 s which corresponded to more than 2000 rotor revolutions. Figure 3 presents typical pressure signal registered during such a procedure. The signal itself allowed to identify certain stages of entering unstable regime. One can observe that the stable working regime was followed by a period $t \in$ (6s; 9s) characterized by increased pressure amplitude accompanied with separate peaks. Then the peaks disappeared, but the amplitude and average value of pressure signal remained higher. Finally, around t = 14 s the onset of high-amplitude oscillations was observed. In this work, the signal was transformed into time-frequency space by means of CWT with Morlet wavelet:

$$CWT(t,s) = \frac{1}{2\pi}\int_{-\infty}^{\infty} X(\omega)\Psi^{in}(\omega)e^{i\omega t}d\omega,$$

where s represents the scaling factor, t – time, ω – frequency, $X(\omega)$ – analysed signal in frequency domain, Fourier transform of the Morlet wavelet has the following form [27]:

$$\Psi(\omega) = \left(4\sigma^2\pi\right)^{\frac{1}{4}} H(\omega)e^{-\frac{1}{2}[\sigma(\omega-\omega_0)]^2},$$

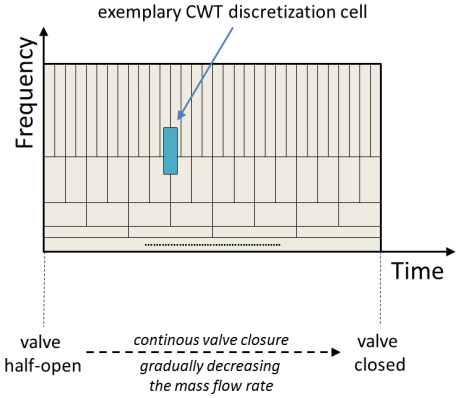

Figure 4: Scheme demonstrating the method used in dynamic tests.

where $\sigma = 1$, $\omega_0 = 6$ and $H(\omega)$ represents the Heaviside step function. The dimensions of the time-frequency atom varied with the frequency as it is presented in Figure 4.

The dynamic method with application of CWT is a widely recognized tool for time-frequency analysis. However, one has to be aware of limitations of such a method:

- Due to Heisenberg-Gabor uncertainty principle, the size of time window was limited [28].
- Resolution in time and frequency domain changed, which made it impossible to satisfy constant uncertainty of the results.

3 Results of study

Figures 5–9 present results of a study conducted based on signals gathered at points p_{s-in}, p_{s-out}, p_{s-imp1}, p_{s-imp2}, p_{s-imp3} respectively. Each figure contains two plots. First represents pressure signals collected in conditions of continuous increment of resistance of the throttling valve. Second contains CWT scalogram obtained on the basis of this signal. The scalograms have a form of colour maps representing amplitude at given time-frequency atom. Due to wide range of analysed frequencies, the vertical axis was presented in the logarithmic scale. Limitations of CWT atom size mentioned in Section 2.2 did not allow for accurate selection of the instantaneous frequency of the signal, especially for its lower values (as presented in Figure 4). Therefore, this method should not be used for precise identification of frequencies of the pressure oscillations. In order to obtain their accurate value one would need to conduct analysis of the stationary signal registered for fixed valve position as it was done in [24]. On the other side, the presented method clearly shows moment of appearance of new frequency components that can be associated with onset of unstable flow phenomena under study.

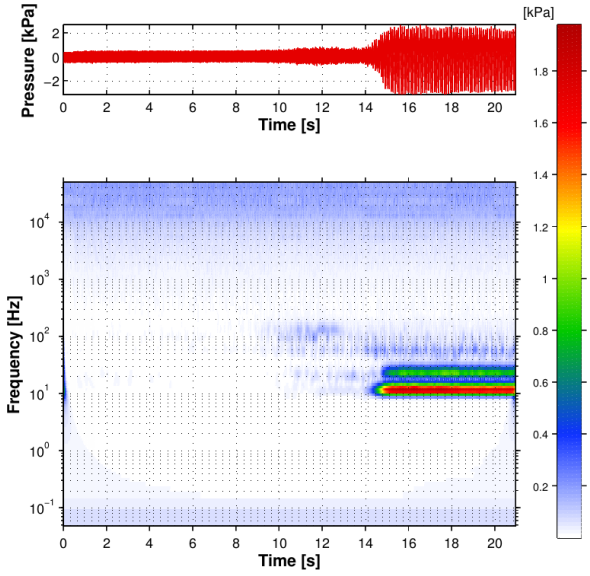

Figure 5: Pressure signal at the gauge p_{s-in} and its CWT scalogram.

The characteristic frequencies detected in the analysis are summarised in Table 1. Based on the character of signal oscillations at all pressure tappings included in this study, four different machine working conditions were identified. Their list is summarized in Table 2 and fully described in Section 4.

4 Discussion

4.1 Inlet

Figure 5 presents the signal registered by the inlet static pressure gauge p_{s-in}. At the beginning, pressure exhibited only slight fluctuations around the atmospheric pressure which did not leave any trace on the CWT scalogram. This region is referred to as the stable regime henceforth. As the time advanced, the throttling valve was closed continuously. One can observe a slight increment in the size of pressure fluctuations at $t \sim 9$ s . It was confirmed by the CWT scalogram that exhibited a slight increment in the amplitude at a wide spectrum of frequencies below and over $f_{rot} = 100$ Hz . This period is referred to as the **transient phase** henceforth. Fluctuations appearing in this regime appeared at $f_3 = 30 \div 100$ Hz and $f_4 = 100 \div 200$ Hz. Very weak fluctuations were also present around $f_1 = 10.2$ Hz and $f_2 = 22$ Hz . Frequency $f_1 = 10.2$ Hz is very close to frequency of the Helmholtz resonator calculated for this machine $f_H = 11.0$ Hz [29]. At $t \sim 14$ s fluctuations increased by one order of magnitude. This was represented on the scalogram by two dis-

Table 1: Characteristic frequencies observed in the dynamic analysis; abbreviations: N-present at a unstable regime, B-present at all conditions.

Notation	Frequency Hz	Type	Gauges	Amplitude kPa	Name
f_{BP}	2300	B	$p_{s-imp2-3}$	various	Blade passing frequency
f_1	10.2	N	all	~ 1	Main surge frequency
f_2	22	N	$p_{s-imp2-3}$	various	
f_3	$30 \div 100$	N	all	$\sim 10^{-1}$	
f_4	$100 \div 200$	N	p_{s-in}, p_{s-out}	$\sim 10^{-1}$	
f_5	$300 \div 1000$	N	p_{s-imp1}	$\sim 10^{-1}$	Inlet recirculation

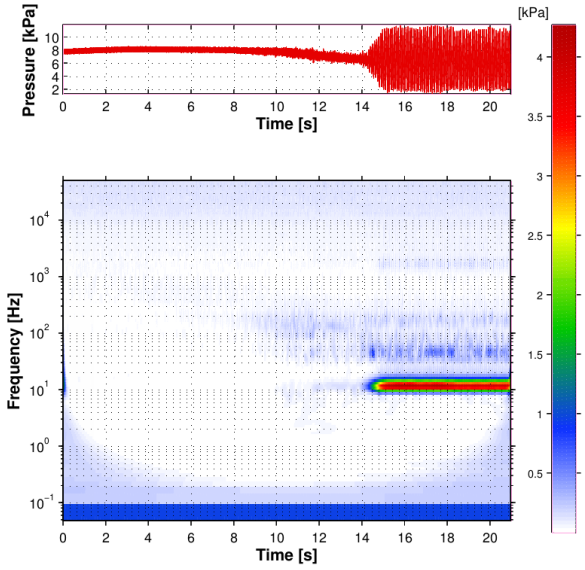

Figure 6: Pressure signal at the gauge p_{s-out} and its CWT scalogram.

tinct pressure peaks that appeared at $f_1 = 10.2$ Hz and $f_2 = 22$ Hz . Smaller fluctuations at $f_3 = 30 \div 100$ Hz remained present. This region is referred to as the **deep surge** henceforth. At all circumstances, weak oscillations were observed at frequencies higher than 10 kHz . Their presence was caused by the signal noise and remained unchanged regardless of the system working regime.

4.2 Outlet

The outlet pressure gauge p_{s-out} registered similar behaviour which is reflected in signal amplitude plot and its CWT scalogram (Figure 6). The main difference came from the dependency of pressure ratio on mass flow rate. This resulted in gradual change of pressure at the outlet. One can observe that the pressure signal resembled the performance curve of the compressor at $t < 14$ s. This variation

Table 2: Working regimes identified based on CWT analysis of signals gathered at all points.

Time range	Stability	Gauges	Name
$t < 6$s	Stable	all	Stable work
$t \in (6\text{s}; 9\text{s})$	Stable	p_{s-imp1}	Inlet recirculation
$t \in (9exts; 14\text{s})$	Unstable	all	Transient phase
$t > 14$s	Unstable	all	Deep surge

of the average outlet pressure resulted in high amplitude at the frequency 10^{-1} Hz observed on the scalogram. When the system entered the deep surge at $t \sim 14$ s one strong pressure peak appeared at $f_1 = 10.2$ Hz. Fluctuations were also observed at $f_3 = 30 \div 100$ Hz, $f_4 = 100 \div 200$ Hz. In comparison to p_{s-in}, the peak $f_2 = 22$ Hz was not observed at the outlet.

4.3 Inlet zone

The inlet zone static pressure gauge p_{s-imp1} exhibited the same behaviour as the p_{s-in} at $t < 6$ s which can be observed in Figure 7. At $t \in (6\text{ s}; 9\text{ s})$ fluctuations were observed in a wide range $f_5 = 300 \div 1000$ Hz. Pressure signal showed that very strong single pressure jumps were also noted during this period. Non-periodic character of these peaks was responsible for the broadband noise observed in the scalogram. Buffaz and Trebinjac presented results of similar analysis conducted on centrifugal compressor stage used in helicopter designed and built by Turbomeca [30]. They have presented power spectral density map of signal gathered upstream of the impeller that could be easily compared to presented study. They have noted a broadband signal amplification of similar shape, which was named as the mild-stall therein.

This phenomenon was also observed by Mizuki and Oosawa who described it as a very thin part-span rotating stall [15]. They have noticed that this phenomenon had

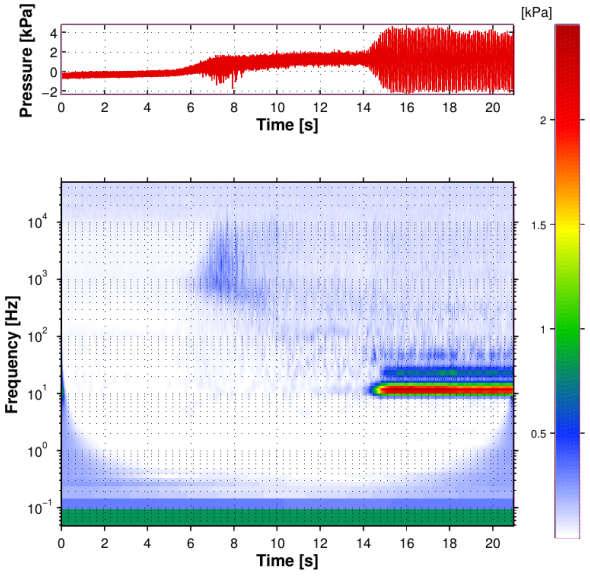

Figure 7: Pressure signal at gauge p_{imp1} and its CWT scalogram.

either no dominating frequency, or the dominating frequency was much higher than those observed by Fringe and Van den Braembussche in reference to progressive impeller rotating stall [vdb]. The flow structure presented by Mizuki and Oosawa had a shape of toroidal recirculation located in vicinity of shroud upstream of the impeller leading edge (Figure 8). Therefore, in this study the nomenclature of McKee *et al.* [23] is applied where this phenomenon was named as the **inlet recirculation**. This name comes from the same flow structure observed in centrifugal pumps by Fraser [13] and Breugelmans and Sen [14].

Pressure jumps were associated with increment of its average pressure which reproduced the results obtained by Bulot *et al.* [18] for a high-speed compressor (pressure ratio 9, rotational speed of 50000 rpm). However, in their study this increment appeared several rotations prior to the deep surge and no long-lasting transient phase was observed. In this case the transient phase $t \in (9\,\text{s}; 14\,\text{s})$ corresponded to 500 rotations of the impeller. During this period signal amplification in regions $f_3 = 30 \div 100$ Hz and $f_4 = 100 \div 200$ Hz appeared. At the deep surge strong peaks were observed at $f_1 = 10.2$ Hz and $f_2 = 22$ Hz which were accompanied by weaker oscillations in the range $f_3 = 30 \div 100$ Hz.

4.4 Impeller

At gauge p_{s-imp2} (Figure 9) the inlet recirculation was also present, but to smaller extent than in the inlet zone. In

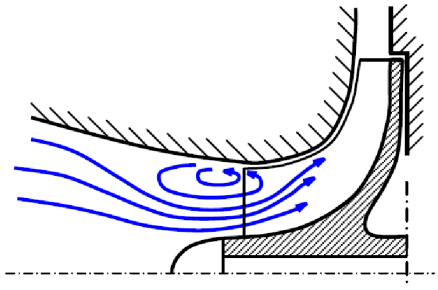

Figure 8: Flow structure of the inlet recirculation (after [13–15]).

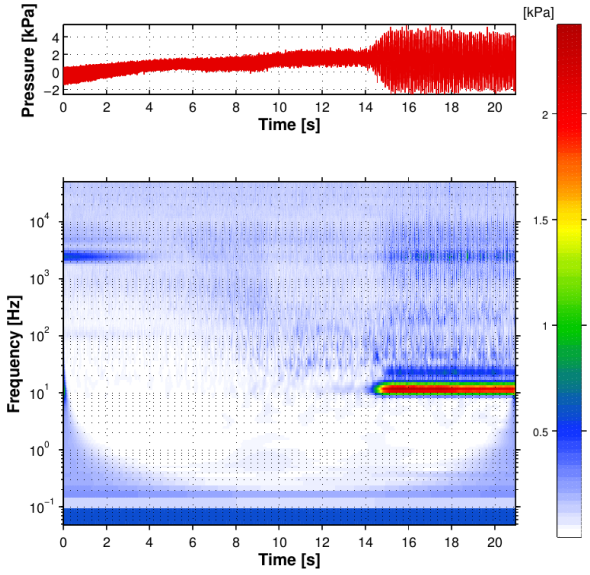

Figure 9: Pressure signal at gauge p_{imp2} and its CWT scalogram.

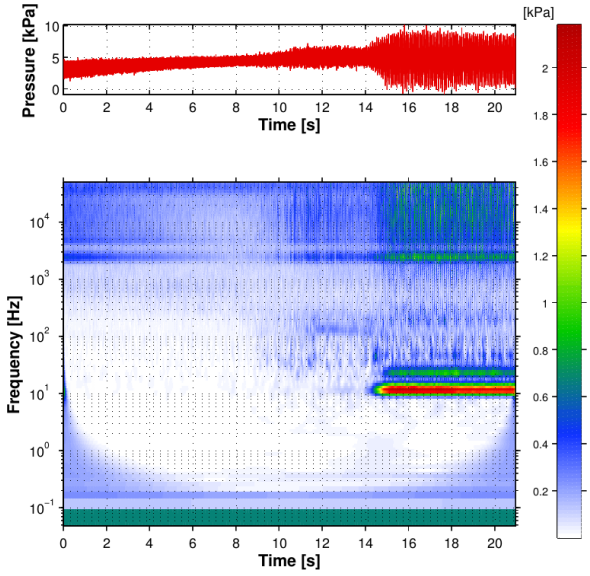

Figure 10: Pressure signal at gauge p_{imp3} and its CWT scalogram.

this case the rise of an average pressure was less noticeable which was in agreement with findings of Bulot *et al.* [18], that the average pressure rise decreases from leading edge to trailing edge. Around $t \sim 9$ s the system entered the transient phase, where the oscillations of frequencies characteristic for the inlet recirculation ($f_5 = 300 \div 1000$ Hz) were weaker. Concurrently, fluctuations appeared at $f_3 = 30 \div 100$ Hz and $f_4 = 100 \div 200$ Hz. At the deep surge, two strong peaks appeared at $f_1 = 10.2$ Hz (main surge frequency) and $f_2 = 22$ Hz. At high frequencies one can observe the peak at the blade passing frequency $f_{PB} = 2.3$ kHz which was caused by pressure drop over blade tips. It diminished for the inlet recirculation and the transient phase.

Gauge p_{s-imp3} was located very close to the blade trailing edge. One can observe in Figure 10, that this location was not affected by the inlet recirculation, as the fluctuations at $t \in (6\,\text{s}; 9\,\text{s})$ did not exhibit character similar to p_{s-imp1} and p_{s-imp2}. At the transient phase, fluctuations were present only at $f_3 = 30 \div 100$ Hz and $f_4 = 100 \div 200$ Hz. At the deep surge, peaks $f_1 = 10.2$ Hz and $f_2 = 22$ Hz appeared as well as wider fluctuations at $f_3 = 30 \div 100$ Hz and $f_4 = 100 \div 200$ Hz. Moreover, during the whole test peak at $f_{PB} = 2.3$ kHz was noticeable.

5 Summary

A time-frequency analysis of low specific speed centrifugal blower was conducted. Static pressure was registered at five locations (inlet, outlet and three points at the shroud) in conditions of continuous closure of the throttling valve. The most important outcomes are listed below:

- First instability in the system was registered upstream of the impeller much before the deep surge. It had a form of strong pressure jumps typical for the inlet recirculation.
- At the later stage, weak oscillations were observed at wide spectrum of frequencies. It was present at all analysed locations, however frequency range of oscillations varied from gauge to gauge.
- At the final stage, the deep surge was initiated. It was characterized by strong oscillations with one dominating frequency $f_1 = 10.2$ Hz registered at all analysed gauges.
- Main frequency at the deep surge was very close to frequency of the Helmholtz resonator $f_H = 11.0$ Hz.

References

[1] Emmons H., Pearson C., Grant H., Compressor surge and stall propagation. Trans. ASME, 1955, 77, 455–467.

[2] Greitzer E., Surge and rotating stall in axial flow compressors-part I: theoretical compression system model. J. Eng. P., 1976, 98, 190–198.

[3] Greitzer E., Surge and rotating stall in axial flow compressors-part II: experimental results and comparison with theory. J. Eng. P., 1976, 98, 199–211.

[4] Meuleman C., Willems F., de Lange R., de Jager B., Surge in a low speed radial compressor, Proceedings of 43rd International Gas Turbine and Aeroengine Congress, ASME, Stockholm, 1998.

[5] Moore F., Greitzer E., A theory of post-stall transients in axial compression systems-part I: development of equations. J Eng. Gas Turb. Power, 1986, 108, 68–76.

[6] Moore F., Greitzer E., A theory of post-stall transients in axial compression systems-part II: application. J Eng. Gas Turb. Power, 1986, 108, 231–239.

[7] Cumpsty N., Compressor aerodynamics. Halsted Press, Cambridge, 1989.

[8] Lennemann E., Howard J., Unsteady ow phenomena in rotating centrifugal impeller passages. J. Eng. P., 1970, 92, 65–71.

[9] Mizuki S., Kawashima Y., Ariga I., Investigation concerning rotating stall and surge phenomena within centrifugal compressor channels. Proceedings of International Gas Turbine Conference, ASME, London, 1978.

[10] Abdelhamid A., Bertrand J., Distinctions between two types of self excited gas oscillations in vaneless radial diffusers. Proceedings of Turbo Expo, ASME, San Diego, 1979.

[11] Jansen W., Rotating stall in a radial vaneless diffuser. J. Basic. Eng.-T. ASME, 1964, 86, 750–758.

[12] Senoo Y., Ishida M., Kinoshita Y., Asymmetric flow in vaneless diffusers of centrifugal blowers. J. Fluid Eng.-T ASME, 1977, 99, 104–111.

[13] Fraser W., Recirculation in centrifugal pumps. Materials of Construction of Fluid Machinery and Their Relationship to Design and Performance, 1981, 1, 65–86.

[14] Breugelmans F., Sen M., Prerotation and fluid recirculation in the suction pipe of centrifugal pumps. Proceedings of 11th International Pump Symposium, A&M University, Texas, 1982.

[15] Mizuki S., Oosawa Y., Unsteady flow within centrifugal compressor channels under rotating stall and surge. J. Turbomach., 1992, 114, 312–320.

[16] Lawless P., Fleeter S., Rotating stall acoustic signature in a low-speed centrifugal compressor-part 1: vaneless diffuser. J. Turbomach., 1995, 117, 87–96.

[17] Horodko L., Investigation of centrifugal compressor surge with wavelet methods, Proceedings of 6-th European Conference on Turbomachinery. Fluid Dynamics and Thermodynamics, VKI, Lile, 2005, 1, 7–11.

[18] Bulot N., Ottavy X., Trebinjac I., Unsteady pressure measurements in a high-speed centrifugal compressor. J. Therm. Sci., 2010, 19, 34–41.

[19] Turunen-Saaresti T., Larjola J., Unsteady pressure field in a vaneless diffuser of a centrifugal compressor: an experimental and computational analysis. J. Therm. Sci., 2004, 13, 302–309.

[20] Tamaki H., Experimental study on surge inception in a centrifugal compressor. IJFMS, 2009, 2, 409–417.

[21] Horodko L., Kryłłowicz W., Investigation of the rotating stall in a centrifugal compressor. ASME Joint US-European Fluids Engineering Conference, Montreal, July 14–18, 2002, 1547–1551.
[22] Horodko L., Identification of rotating pressure waves in a centrifugal compressor diffuser by means of the wavelet cross-correlation. Int. J. Wavelets Multi., 2006, 4, 373–382.
[23] Mckee R., Deffenbaugh D., Increased flexibility of turbo-compressors in natural gas transmission through direct surge control. Technical Report, Southwest Research Institute, San Antonio, 2003, doi:10.2172/823041.
[24] Liśkiewicz G., Horodko L., Stickland M., Kryłłowicz W., Identification of phenomena preceding blower surge by means of pressure spectral maps. Exp. Therm. Fluid Sci., 2014, 54, 267–278.
[25] Kuzmin V., Khazhuev V., Measurement of liquid or gas flow (flow velocity) using convergent channels with a Witoszynski profile, Meas. Tech.+, 1993, 36, 288-296.
[26] Fink D., Cumpsty N., Greitzer E., Surge dynamics in a free-spool centrifugal compressor system. J. Turbomach., 1992, 114, 321–332.
[27] Horodko L., Zastosowanie czasowo-częstotliwościowej analizy sygnałów do badania niestatecznej pracy sprężarki promieniowej. Technical Report 990, Lodz University of Technology, 2006.
[28] Mertins A., Signal Analysis: Wavelets, Filter Banks, Time-Frequency Transforms and Applications. Wiley Press, Chichester, 1999.
[29] Kabalyk K., Liśkiewicz G., Horodko L., Stickland, M., Kryłłowicz W., Use of pressure spectral maps for analysis of influence of the plenum volume on the surge in centrifugal blower. Proceedings of Turbo Expo, ASME, Düsseldorf, 2014.
[30] Buffaz N., Trebinjac I.. Aerodynamic instabilities in transonic centrifugal compressor. Mech. Ind., 2014, 15, 191–196.